



## OPEN ACCESS

## EDITED BY

Jonathan Y.S. Leung,  
University of Adelaide, Australia

## REVIEWED BY

Eva Chatzinikolaou,  
Hellenic Centre for Marine  
Research, Greece  
Xinqing Zheng,  
State Oceanic Administration, China

## \*CORRESPONDENCE

Casey P. Saenger  
✉ saengec@www.edu

## SPECIALTY SECTION

This article was submitted to  
Global Change and the Future Ocean,  
a section of the journal  
Frontiers in Marine Science

RECEIVED 10 November 2022

ACCEPTED 23 January 2023

PUBLISHED 10 February 2023

## CITATION

Saenger CP, McElhany P, Norton EL,  
Busch DS, Siedlecki SA, Alin SR, Feely RA,  
Hermann AJ and Bednaršek N (2023)  
Evaluating environmental controls on the  
exoskeleton density of larval Dungeness  
crab *via* micro computed tomography.  
*Front. Mar. Sci.* 10:1095253.  
doi: 10.3389/fmars.2023.1095253

## COPYRIGHT

© 2023 Saenger, McElhany, Norton, Busch,  
Siedlecki, Alin, Feely, Hermann and  
Bednaršek. This is an open-access article  
distributed under the terms of the [Creative  
Commons Attribution License \(CC BY\)](#). The  
use, distribution or reproduction in other  
forums is permitted, provided the original  
author(s) and the copyright owner(s) are  
credited and that the original publication in  
this journal is cited, in accordance with  
accepted academic practice. No use,  
distribution or reproduction is permitted  
which does not comply with these terms.

# Evaluating environmental controls on the exoskeleton density of larval Dungeness crab *via* micro computed tomography

Casey P. Saenger<sup>1\*</sup>, Paul McElhany<sup>2</sup>, Emily L. Norton<sup>3</sup>,  
D. Shallin Busch<sup>2</sup>, Samantha A. Siedlecki<sup>4</sup>, Simone R. Alin<sup>5</sup>,  
Richard A. Feely<sup>5</sup>, Albert J. Hermann<sup>3,5</sup> and Nina Bednaršek<sup>6,7</sup>

<sup>1</sup>Department of Geology and Program in Marine and Coastal Science, Western Washington University, Bellingham, WA, United States, <sup>2</sup>Conservation Biology Division, Northwest Fisheries Science Center, National Marine Fisheries Service, National Oceanic and Atmospheric Administration, Seattle, WA, United States, <sup>3</sup>The Cooperative Institute for Climate, Ocean and Ecosystem Studies, University of Washington, Seattle, WA, United States, <sup>4</sup>Department of Marine Sciences, University of Connecticut Groton, Groton, CT, United States, <sup>5</sup>Pacific Marine Environmental Laboratory, National Oceanic and Atmospheric Administration, Seattle, WA, United States, <sup>6</sup>Cooperative Institute for Marine Resources Studies, Oregon State University, Newport, OR, United States, <sup>7</sup>National Institute of Biology, Marine Biological Station, Piran, Slovenia

Dungeness crab (*Metacarcinus magister*) have significant socioeconomic value, but are threatened by ocean acidification (OA) and other environmental stressors that are driven by climate change. Despite evidence that adult harvests are sensitive to the abundance of larval populations, relatively little is known about how Dungeness megalopae will respond to these stressors. Here we evaluate the ability to use micro-computed tomography ( $\mu$ CT) to detect variations in megalope exoskeleton density and how these measurements reflect environmental variables and calcification mechanisms. We use a combination of field data, culture experiments, and model simulations to suggest resolvable differences in density are best explained by minimum pH at the time zoeae molt into megalopae. We suggest that this occurs because more energy must be expended on active ion pumping to reach a given degree of calcite supersaturation at lower pH. Energy availability may also be reduced due to its diversion to other coping mechanisms. Alternate models based on minimum temperature at the time of the zoea-megalope molt are nearly as strong and complicate the ability to conclusively disentangle pH and temperature influences. Despite this, our results suggest that carryover effects between life stages and short-lived extreme events may be particularly important controls on exoskeleton integrity.  $\mu$ CT-based estimates of exoskeleton density are a promising tool for evaluating the health of Dungeness crab populations that will likely provide more nuanced information than presence-absence observations, but future *in situ* field sampling and culture experiments are needed to refine and validate our results.

## KEYWORDS

crab, megalopa larvae, zoea larva, computed tomography, exoskeleton density, ocean acidification

# 1 Introduction

Dungeness crab (*Metacarcinus magister*) support the most valuable single-species fishery on the US West Coast (Pacific States Marine Fisheries Commission, 2019) and are an important traditional food source for indigenous populations (Ban et al., 2017). Their habitat range spans cool oceans from Alaska to southern California (Rasmuson, 2013), which are vulnerable to anthropogenic ocean acidification (OA) due to naturally low seawater buffering capacity in portions of the region (Feely et al., 1988; Feely et al., 2016; Chavez et al., 2017). While the Dungeness crab fishery may currently be sustainable (Richerson et al., 2020), model projections suggest accelerating OA (Chan et al., 2017; Doney et al., 2020) will lead to future declines and considerable socioeconomic impacts, especially in Oregon and Washington (Marshall et al., 2017; Hodgson et al., 2018; Magel et al., 2020; Berger et al., 2021). However, these model projections are based on relatively limited physiological data with only modest agreement among studies (Busch and McElhany, 2016), indicating that additional work is necessary to robustly characterize the response of Dungeness crabs to OA and other stressors associated with anthropogenic climate change.

Of particular importance may be the response of larval stages. The life cycle of Dungeness crabs includes five zoeal stages (z1-z5) and a single megalopal stage during which active swimming and passive transport lead to migration from nearshore environments to the open ocean and back over the course of approximately four months (Rasmuson, 2013). In the northern California Current, these pelagic stages experience a range of environmental conditions, especially during the spring upwelling season when any onshore transport exposes them to lower pH, dissolved oxygen (DO), and temperature. The size of the adult commercial catch in a given year has been linked to the abundance of megalopae four years earlier (Shanks and Roegner, 2007; Park, 2012; Shanks, 2013) suggesting that understanding how megalopae respond to OA and other environmental stressors such as low DO and non-optimal temperature is critical for understanding potential impacts on the adult population.

Evidence from laboratory experiments suggests that the growth, survival, and physiology of megalopae are sensitive to temperature (Reed, 1969; Sulkin and McKeen, 1994; Sulkin et al., 2011, 1989; Wild, 1980), salinity (Reed, 1969; Brown and Terwilliger, 1999) and DO (Bancroft, 2015; Gossner, 2018; Trigg et al., 2019). These results are partially corroborated by field observations that suggest megalope abundance is sensitive to salinity (Lough, 1976) and the Pacific Decadal Oscillation (Hobbs and Botsford, 1992; Shanks and Roegner, 2007; Shanks, 2013). Experiments evaluating responses of Dungeness crab to OA indicate that low pH may reduce survival and slow development (Descôteaux, 2014; Miller et al., 2016), affect behavioral and cognitive abilities (Christmas, 2013; Imm, 2015), and reduce carapace size and respiration rate (McElhany et al., 2022). Similar experiments with larval stages of other crab species also suggest lower growth and survival (Walther et al., 2010; Giltz and Taylor, 2017; Gravinese et al., 2018), decreased metabolism (Long et al., 2016) and altered vertical migration (Gravinese et al., 2019). However, a long-term study on juvenile Dungeness crabs found increased survival under high  $p\text{CO}_2$  conditions, suggesting that the response may be life stage dependent (McElhany et al., 2022).

Relatively few field observations have investigated the response of Dungeness crab megalopae to carbonate chemistry conditions, perhaps because carbonate chemistry data are spatiotemporally sparse relative to other environmental variables. A notable exception is the recent work of Bednaršek et al. (2020) who used data from NOAA's 2016 West Coast Ocean Acidification (WCOA) cruise to relate dissolution in the exoskeleton of Dungeness crab megalopae to *in situ* ocean variables that included carbonate chemistry metrics. Results found that the extent of external carapace dissolution, including damage to important mechanoreceptors, was highly correlated with the vertical gradient in calcite saturation over the upper 60 m of the water column ( $\Delta\Omega_{60}$ ). In addition to providing important evidence that OA is influencing megalopae under present-day conditions, Bednaršek et al. (2020) study is noteworthy for developing an OA vulnerability metric that is more nuanced than simple mortality rates or presence-absence observations (e.g. Miller et al., 2016; Gravinese et al., 2018). Such non-binary metrics allow the consequences of exposure to be evaluated across a spectrum, and may contribute to more detailed forecasts of Dungeness crab population response to future climate change (e.g. Berger et al., 2021). However, because the technique targets dissolution, it emphasizes damage between molts and may miss processes that affect initial megalope exoskeleton integrity at the time of molt from the fifth zoeal stage (z5). Furthermore, observed exoskeleton dissolution has not been linked to survival, growth or other parameters that can be directly related to changes in population dynamics.

Unlike the many marine organisms that secrete carbonate biominerals more continuously, crabs precipitate their exoskeleton in short, episodic molts with no new shell formed during intermolts (Luquet, 2012). While exoskeleton formation in larval crabs is poorly constrained, adult crabs shed their old shells and precipitate new ones in a matter of hours *via* a number of energetically-intensive active processes aimed at elevating mineral saturation states while maintaining charge and acid-base balance (Cameron, 1985, 1989; Cameron and Wood, 1985; Luquet and Marin, 2004). Thus, it is plausible that variations in carbonate chemistry, food availability and other environmental variables during the brief z5 to megalope transition could lead to initial variations in exoskeleton density. Subsequent dissolution between the time of initial exoskeleton precipitation and collection could then further modify density.

Micro-computed tomography ( $\mu\text{CT}$ ) represents a complement to the work of Bednaršek et al. (2020) that may be able to provide additional information on how megalopae respond to OA and other stressors during molt and intermolt stages by measuring exoskeleton mineral density. The technique is relatively fast, nondestructive, and provides objective data that are well suited to high throughput and routine monitoring. While often used to evaluate three-dimensional structures in marine calcifiers (Saenger et al., 2009; Cantin et al., 2010; Enochs et al., 2016; Johnson et al., 2020; Mekkes et al., 2021) the degree of x-ray attenuation also allows  $\mu\text{CT}$  to measure the density of those structures. Applying such measurements to culture experiments in which carbonate chemistry is manipulated suggests that the shell densities of oysters (Meng et al., 2018), gastropods (Chatzinikolaou et al., 2021, 2017) and scallops (Alma et al., 2020) decrease under lower pH conditions or high  $p\text{CO}_2$ , while the density of fish otoliths and bone increases at high  $p\text{CO}_2$  (Bignami et al., 2013; Di Santo, 2019). *In situ* field studies more realistically represent the true

environment of marine calcifiers, but are often more difficult to interpret because of the potential for confounding variables. For example, the density of foraminifera (Iwasaki et al., 2019) and thickness of pteropod shells (Mekkes et al., 2021) in some regions show a decrease at lower carbonate ion concentrations, while in other regions the density of both organisms shows the opposite trend (Ofstad et al., 2021). This highlights the need to carefully consider as many realistic controls on exoskeleton density as possible when evaluating  $\mu$ CT-based density as a measure of the sensitivity of Dungeness crab megalopae to carbonate chemistry conditions.

Here, we develop a rapid-throughput  $\mu$ CT technique to measure exoskeleton density variations among Dungeness crab megalopae collected during the 2016 WCOA cruise and complementary cultured larval pea crabs. We evaluate the environmental variables that are most likely to control differences in exoskeleton density by comparing variations among megalopae to *in situ* ocean observations, exoskeleton dissolution estimates (Bednaršek et al., 2020), and corresponding simulated megalope exposure histories from the same time period (Norton et al., 2020). These analyses are used to develop plausible mechanisms linking exoskeleton formation to environmental variables, and to make an initial evaluation of how the responses at the individual level may translate to larger populations.

## 2 Methods

### 2.1 Megalopae and water sampling

Megalopae were collected during the NOAA WCOA cruise in May and June of 2016 (Figure 1; Table 1). Neuston and Bongo nets with a mesh size of 333 mm were deployed obliquely across a depth of ~60m, which spans the vertical habitat of larval Dungeness crabs (Hobbs and Botsford, 1992; Rasmuson, 2013) for a duration of approximately 20 minutes. Megalopae were sampled from tow samples and stored in 100% non-denatured ethanol for later

TABLE 1 Station locations and mean densities of megalopae.

station	lat.	lon.	dist. to shore (km)	n individuals	greyscale density
94	46.13	-124.67	46.45	7	14.61
99	47.12	-124.64	32.71	13	15.72
100	47.12	-124.82	44.72	13	16.83
106	47.96	-125.33	49.21	10	14.64
114	48.86	-125.42	3.72	11	15.47
115	48.84	-125.46	6.64	13	16.14
120	48.54	-126.00	54.93	8	14.88
127	51.83	-130.37	46.21	10	13.93
130	52.4	-129.05	6.72	13	15.20

analysis. The distance to shore for each station was estimated using the closest 0.04° gridbox from the NASA Ocean Biology Processing Group's product (<https://oceancolor.gsfc.nasa.gov/docs/distfromcoast/>).

Complementary water column variables were collected across vertical profiles at each site including: temperature (T), salinity (S), DO, nitrate (NO<sub>3</sub><sup>-</sup>) and phosphate (PO<sub>4</sub><sup>3-</sup>) concentrations, total dissolved inorganic carbon (TC), alkalinity and pH (measured at 25°C - corrected to *in situ* temperature, and expressed on the total pH scale). Subsequently, seawater calcite saturation state ( $\Omega_c$ ) was calculated using CO2SYS as described by Feely et al. (2016). At most stations, water data exist at approximately 10-m intervals over at least the upper 60 m approximating megalope habitat. However, the maximum water sampling depth at nearshore stations 114 and 130 was 35 and 41 m, respectively.

### 2.2 $\mu$ CT analysis

Megalopae were scanned using a Bruker Skyscan 1173 within the Karel F. Liem Bioimaging Facility at the University of Washington's Friday Harbor Laboratories. While  $\mu$ CT could be used to measure a variety of exoskeleton metrics (e.g. volume, shell thickness, etc.), our method was optimized for the high throughput analysis of exoskeleton density with the hope that such measures become a routine component of marine monitoring. Between 2 and 4 megalopae were loaded dry into a plastic 2 ml vial and scanned simultaneously in air without a filter at a voltage of 49 kV, current of 160 mA and 0.3° rotation steps. Total time for each scan was less than 30 minutes, or approximately 10 minutes per megalope. The raw output of each scan was a histogram of greyscale values from 0 (black) to 255 (white), for which higher values indicate greater density. Scans from the same station were aggregated into an average histogram for that site representing 7 to 13 specimens (Table 1).

The megalope greyscale signal in each histogram is convolved with the background signal of the plastic vial, which must be removed (Figure 2). To achieve this, we identified the first greyscale value whose proportion increases from the previous value as the lower limit of the megalope signal and the first subsequent greyscale value whose proportion is <0.1% of the total as the upper limit (Figure 2). We then

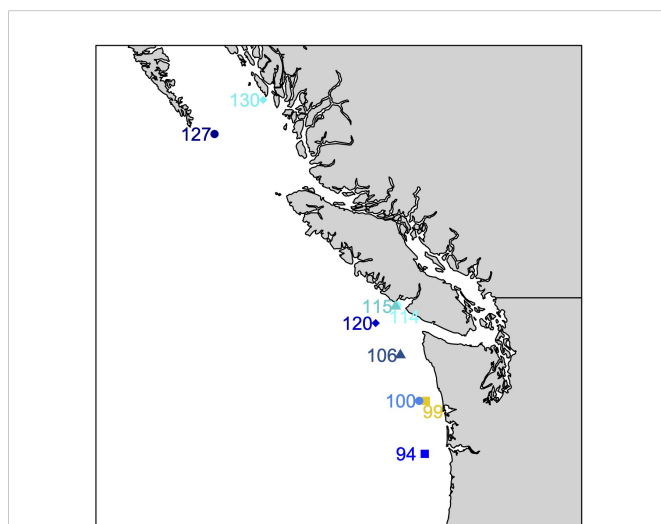
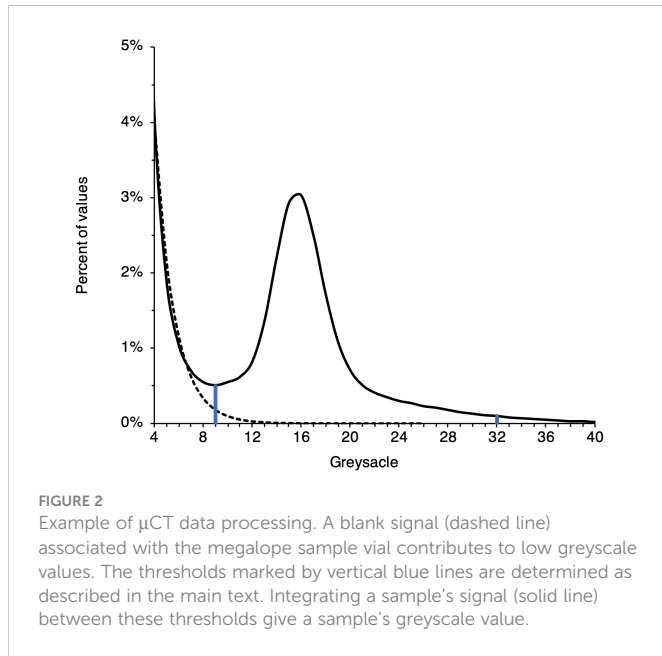


FIGURE 1 Locations of megalope sampling stations. Blue and cyan symbols identify offshore (>50 km from shore) and nearshore (<7 km) stations, respectively. Station 99 (yellow) is intermediate (33 km from shore).



integrated between these values to determine a final greyscale value for each site. Given that the exoskeleton of megalopae are likely a complex mixture of calcite, amorphous calcium carbonate, and chitin (Luquet and Marin, 2004; Boßelmann et al., 2007), with densities of 2.71 g/cm<sup>3</sup>, 1.62 g/cm<sup>3</sup> (Bolze et al., 2002), and 1.4 g/cm<sup>3</sup> (Carlstrom, 1957), respectively, it is difficult to produce appropriate standards with which to convert greyscale values to absolute density. Furthermore, while higher greyscale values generally reflect denser material, the abundance of exoskeleton pores smaller than the ~20 mm resolution of our method (i.e., micropores) can complicate this relationship. To compute density from a  $\mu$ CT scan, it is necessary to identify a threshold value that separates mineral or exoskeleton from air (Meng et al., 2018; Fordyce et al., 2020). A high abundance of micropores increases the number of voxels that are not entirely exoskeleton or air; a phenomenon known as ‘partial voxel filling’ (Fordyce et al., 2020). The higher the frequency of partial voxel filling,

the greater the likelihood that voxels of mostly air with a small proportion of high-density exoskeleton are identified as entirely low-density exoskeleton. Given these complications, we do not attempt to calibrate  $\mu$ CT data to absolute density, and instead present data in native greyscale units.

### 2.3 Optimal predictors of megalope exoskeleton density

The environmental variables that may control differences in megalope exoskeleton density were evaluated by comparing density to a suite of plausible predictors that represent realistic megalope histories prior to collection. These scenarios are summarized in Table 2. In the simplest scenarios (int30 and int60), it was assumed that the recovered specimens molted from z5 zoeae near the point of collection such that the environmental conditions measured at the time of sampling were representative of their entire history as megalopae. In these scenarios we considered vertical migrations over either the upper 30 or 60 m, which is broadly consistent with field observations (Hobbs and Botsford, 1992; Rasmuson, 2013). The predictor pool for these scenarios included T, S, DO, NO<sub>3</sub><sup>-</sup>, PO<sub>4</sub><sup>3-</sup>, TC, alkalinity, pH and  $\Omega_c$  averaged over depths of either 30 m or 60 m. For select instances where a station's maximum depth was less than 60 m, data at the maximum available depth was used. To consider particular sensitivity to extreme values, we also considered the maximum and minimum of the variables over either the upper 30 or 60 m. Given recent work suggesting that megalope carapace dissolution is sensitive to vertical gradients in  $\Omega_c$  (Bednaršek et al., 2020), we also added such gradients for T, S and  $\Omega_c$  ( $\Delta T$ ,  $\Delta S$ ,  $\Delta\Omega_c$ ), where the  $\Delta$ -value is the difference between the parameter at the surface and 30 m or 60 m.

In a second set of scenarios (DVM30<sub>xx</sub> and DVM60<sub>xx</sub>), we considered the possibility that megalopae molted from z5 zoeae up to 30 days prior to collection, and experienced environmental conditions different from *in situ* measurements as they migrated to the sampling site. Because megalopae are active swimmers, we

TABLE 2 Summary of scenarios considered.

Name	Summary	Stations (n)	Predictors considered
int30	megalopae migrate over the upper 30 m, and conditions at the time of collection are representative of their history as megalopae	94, 99, 100, 106, 114, 115, 120, 127, 130	mean of: T, S, DO, NO <sub>3</sub> , PO <sub>4</sub> , TC, alk, [CO <sub>3</sub> ], pH $\Omega$ , Chla, pCO <sub>2</sub> . max and min of: T, S, DO, NO <sub>3</sub> , PO <sub>4</sub> , TC, alk, [CO <sub>3</sub> ], pH $\Omega$ , Chla, pCO <sub>2</sub> . $\Delta T$ , $\Delta S$ , $\Delta\Omega$
int60	as above, but megalopae migrate over the upper 60 m	as above	as above, but over the upper 60 m
DVM30 <sub>xx</sub>	megalopae molt 10, 20 or 30 days before collection (noted by subscript), and experience diel vertical migrations through the upper 30 m.	94, 99, 100, 106, 114, 115, 120	mean of: T, S, DO, [phyt], NO <sub>3</sub> , pH $\Omega$ . max and min of: T, S, DO, [phyt], NO <sub>3</sub> , pH $\Omega$ . severity index of: T, S, DO, pH $\Omega$ . $\Delta T$ , $\Delta S$ , $\Delta\Omega$
DVM60 <sub>xx</sub>	as above, but diel vertical migrations over the upper 60 m	as above	as above, but over the upper 60 m
molt30 <sub>xx</sub>	carapace density is set at the time of z5-megalope molt; 10, 20 or 30 days before collection (noted by subscript)	as above	mean of: T, S, DO, [phyt], NO <sub>3</sub> , pH $\Omega$ . max and min of: T, S, DO, [phyt], NO <sub>3</sub> , pH $\Omega$ .
molt60 <sub>xx</sub>	as above, but megalopae migrate over the upper 60 m	as above	as above, but over the upper 60 m
all30 <sub>xx</sub>	conditions at molt, migration to, and at, the point of collection could influence density. Molt 10, 20 or 30 days before collection noted by subscript	as above	combined predictors from int30, DVM30 and molt30.
all60 <sub>xx</sub>	as above, but megalopae migrate over the upper 60 m	as above	combined predictors from int60, DVM60 and molt60.

considered diel vertical migrations over the upper 30 m in DVM30<sub>xx</sub> scenarios and over the upper 60 m in DVM60<sub>xx</sub> scenarios. The total time between z5-megalope molt and subsequent megalope-juvenile molt has been previously estimated at 30 days (Norton et al., 2020), but the exact time between z5-megalope molt and collection for the specimens we analyzed is unknown. Because of this uncertainty we performed sensitivity tests that assumed z5-megalope molt occurred 10, 20 or 30 days prior to collection. These scenarios are distinguished with a subscript, such that DVM30<sub>10</sub> identifies the scenario where the z5-megalope molt occurred 10 days prior to collection, after which megalope migrate over the upper 30 m of the water column to the site of collection.

To evaluate these scenarios we leveraged a series of existing experiments that used JISAO's Seasonal Coastal Ocean Prediction of the Ecosystem (J-SCOPE) model to explore how exposure histories influence the presence or absence of *M. magister* (Norton et al., 2020). J-SCOPE is a high-resolution biogeochemical model of Washington-Oregon shelf waters with demonstrable predictive skill on seasonal timescales (Siedlecki et al., 2016), which has been extensively evaluated against historical conditions (Malick et al., 2020; Norton et al., 2020). Running the model "in reverse" using hourly historical simulations allows a megalope's trajectory to the site of collection to be estimated, and, in turn, record the ocean conditions that coincide with that trajectory (Norton et al., 2020). One hundred particles for each sampling station were considered and the mean of the environmental conditions experienced by the particles was taken as the best estimate for a site. Diel vertical migrations were incorporated into back-tracking experiments, assuming a maximum depth of 30 m (DVM30<sub>xx</sub>; Figure 3) or 60 m (DVM60<sub>xx</sub>; Figure 4). The back-tracked trajectories include both vertical and horizontal random walk terms based on diffusion. The vertical component is calculated using the time-variable, hourly stored 3D values of vertical diffusivity, while the horizontal component assumes a constant background diffusivity value of 1.0 m<sup>2</sup>/s. These terms ensure dispersion of particles released from a shared location. The following variables estimated by J-SCOPE were considered as predictors of greyscale density: T, S, DO, NO<sub>3</sub><sup>-</sup>, pH, Ω<sub>c</sub>, phytoplankton concentration ([phyt]), and their maximum and minimum values, plus ΔT, ΔS and ΔΩ<sub>c</sub>. Maximum and minimum values were defined as the average of the highest and lowest 5% of values for each variable. Following Norton et al. (2020), we also calculated severity indices (SI: Hauri et al., 2013; Bednaršek et al., 2017) for T, S, DO, pH and Ω<sub>c</sub>. Stations 127 and 130 fall outside of the J-SCOPE domain, so comparisons to DVM behaviors were limited to the remaining seven stations.

In a third set of scenarios (molt30<sub>xx</sub> and molt60<sub>xx</sub>), we modeled the possibility that megalope exoskeleton density was determined only by environmental conditions during the short period surrounding the z5-megalope molt, 10, 20 or 30 days prior to collection. To do so, we considered only the final 24 hours of the DVM30<sub>xx</sub> and DVM60<sub>xx</sub> exposure history simulations described above. We considered all depths to be equally likely for the z5-megalope molt and calculated average values of T, S, DO, NO<sub>3</sub><sup>-</sup>, pH, Ω<sub>c</sub>, [phyt], and their maximum and minimum values. We did not consider vertical gradients or severity indices in this set of scenarios. As above, these scenarios were limited to the seven stations within the J-SCOPE domain.

Our final scenarios (all30<sub>xx</sub> and all60<sub>xx</sub>) considered the possibility that the scenarios above are not mutually exclusive. For example,

conditions at the time of z5-megalope molt and the exposure history between molt and collection could both influence density. Thus, we combined the predictors of the three other scenarios at each depth (e.g. int30, DVM30<sub>xx</sub> and molt30<sub>xx</sub>) for the seven stations within the J-SCOPE domain into a single pool.

For each scenario, we used a forward stepwise regression approach (Wilks, 2006; Saenger and Evans, 2019), in which the Akaike Information Criterion (Akaike, 1974) modified for small samples (AICc; Burnham and Anderson, 2010; Burnham et al., 2011), served as a stop criterion. Specifically, univariate regressions between μCT greyscale and all potential predictors were calculated, and the regression with the lowest AICc was retained. Subsequently, all bivariate regressions were calculated. If a bivariate model had a still lower AICc, the additional variable was retained, and the process continued. If no bivariate model had a lower AICc, the univariate model was considered to be optimal. Given the absence of data to the contrary, we assume a linear relationship between greyscale density and all potential predictors. Multicollinearity undoubtedly occurs within our pool of predictor variables and complicates the selection of a single regression with absolute certainty. As such, we present AICc values for all models (See Supplementary Material) and use the difference from the lowest AICc (ΔAICc) to calculate relative likelihoods following the approach of Burnham et al. (2011). We formally discuss models whose likelihoods are >0.5, which is equivalent to a ΔAICc of 1.4, and can be interpreted as the optimal model being at most twice as likely as an alternate model. Furthermore, we provide comprehensive correlation matrices for all variables in each scenario to evaluate the degree to which our stepwise regression selects unique predictors (See Supplementary Material).

Finally, we give special attention to the relationship between greyscale density and exoskeleton dissolution. In a prior study, a subset of the same field-collected samples analyzed here showed evidence for dissolution that likely occurred after the time of z5-megalope molt, but before field collection (Bednaršek et al., 2020). As mentioned above, more severe dissolution was found at sampling locations with steeper vertical gradients in calcite saturation state (ΔΩ<sub>c-60</sub>), and was suggested to be a short-term OA coping mechanism. Given that dissolution has been shown to decrease μCT -based density estimates in other marine calcifiers (Iwasaki et al., 2019), it would not be unreasonable to expect a strong correlation between either the semi-quantitative dissolution estimates of Bednaršek et al. (2020) or ΔΩ<sub>c-60</sub> and our greyscale density data.

## 2.4 Experimental evaluation of pCO<sub>2</sub>

Given multicollinearity among potential environmental predictors, we also attempted to isolate the influence of pCO<sub>2</sub> on megalope exoskeleton density through a controlled experiment with pea crabs (*Pinnixa* sp.). While Dungeness megalopae would have been preferable for this test, attempts to culture the species from the egg to the megalope stage were unsuccessful, at which point wild-caught zoeae were not present in the regional environment. Given that pea crabs and Dungeness crabs are both Eubranchyuran crustaceans and that the larvae can occur in similar habitats, it seems plausible that their biomineralization strategies might also be similar and these

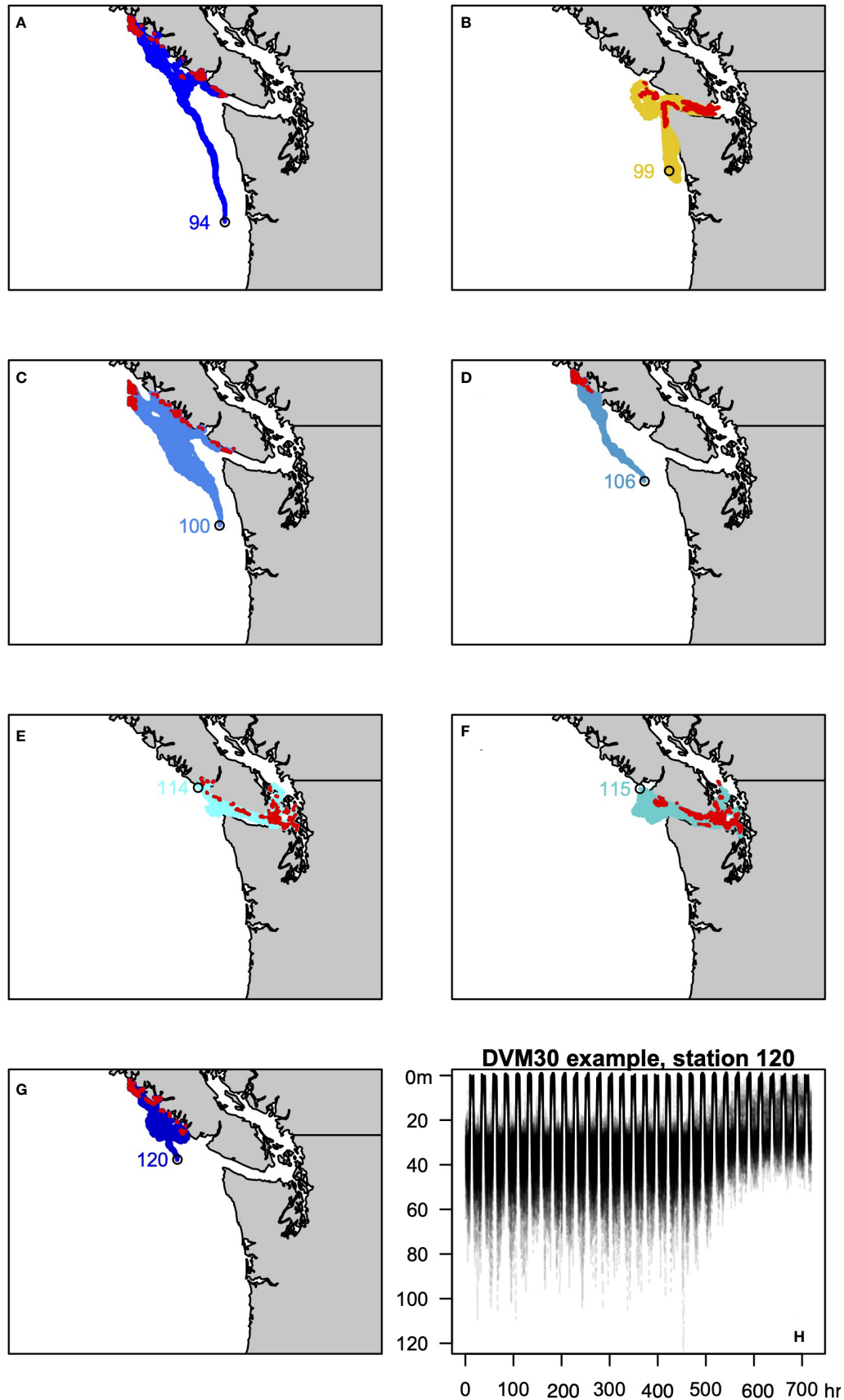


**FIGURE 3**  
**(A–G)** Trajectories of the 100 backtracked particles at each site for the DVM30<sub>30</sub> behavior. Red symbols identify the location in the last 24 hours used to approximate the site of z5-megalope molt 30 days prior to collection. **(H)** Example of DVM30<sub>30</sub> behavior for station 120, showing the depth of all 100 particles over the course of the 720 hour simulation.

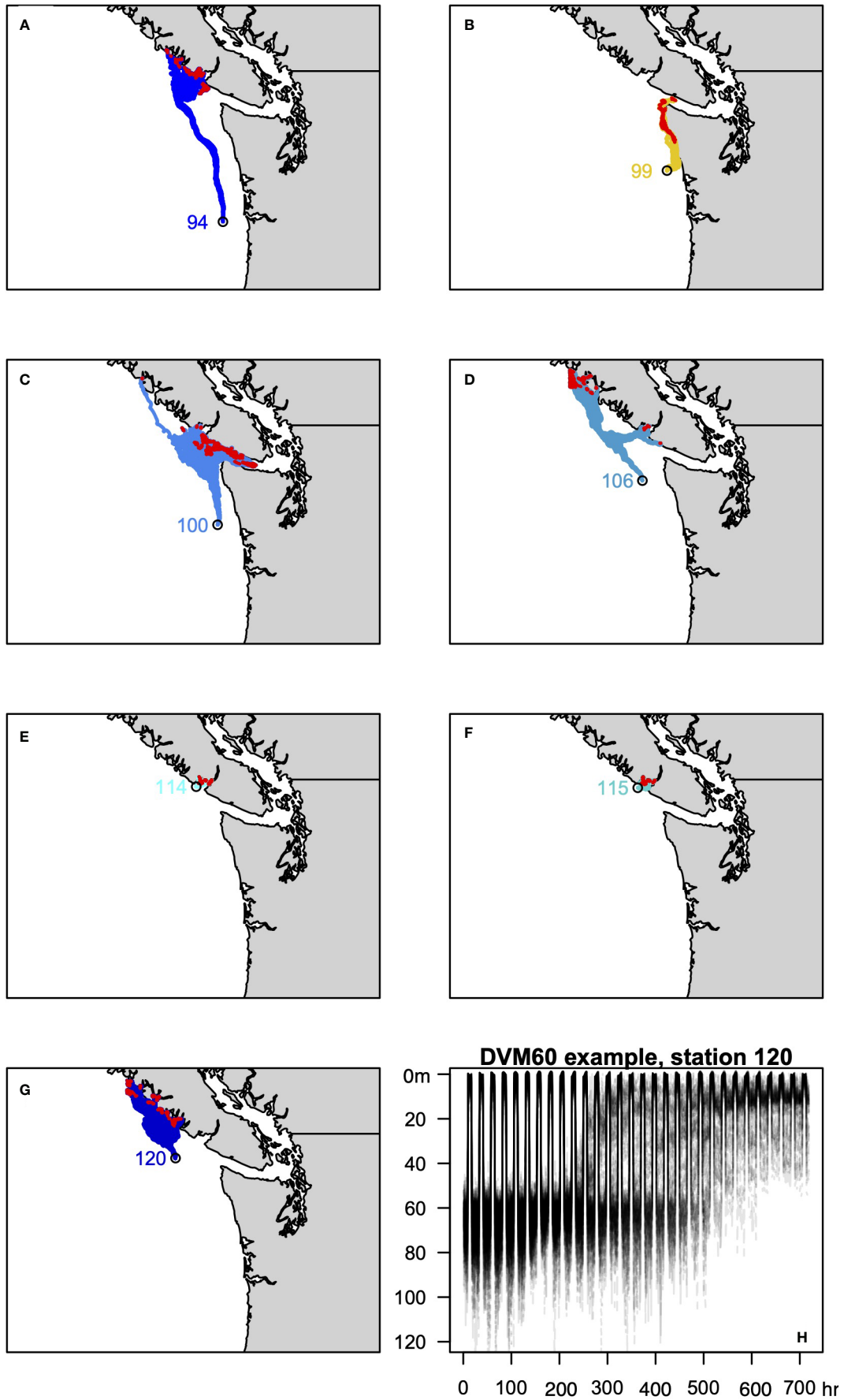


FIGURE 4  
As in Figure 3 for the DVM60<sub>30</sub> behavior.

TABLE 3 Best models of greyscale (gs) for each scenario.

Scenario	Equation	AICc	r <sup>2</sup>	p	n
int30	gs = 0.012*DOmax <sub>in-situ</sub> + 11.50	26.70	0.50	0.03	9
int60	gs = 0.012*DOmax <sub>in-situ</sub> + 11.50	26.70	0.50	0.03	9
DVM30 <sub>10</sub>	gs = -0.53*Ωmin <sub>DVM</sub> + 16.14	28.88	0.17	0.36	7
DVM30 <sub>20</sub>	gs = -2.1*ΔT <sub>DVM</sub> + 22.49	28.83	0.18	0.35	7
DVM30 <sub>30</sub>	gs = 0.45*Tmin <sub>DVM</sub> + 22.49	27.90	0.28	0.22	7
DVM60 <sub>10</sub>	gs = -1.67*Ωmin <sub>DVM</sub> + 16.54	24.22	0.57	0.05	7
DVM60 <sub>20</sub>	gs = 16.01*pHmax <sub>DVM</sub> - 116.8	25.28	0.5	0.07	7
DVM60 <sub>30</sub>	gs = 18.32*pHmax <sub>DVM</sub> - 135.0	23.33	0.6	0.04	7
molt30 <sub>10</sub>	gs = 0.014*DOmax <sub>molt</sub> + 11.04	28.89	0.17	0.36	7
molt30 <sub>20</sub>	gs = 5.28*[phyt]min <sub>molt</sub> + 15.11	28.54	0.21	0.30	7
<b>molt30<sub>30</sub></b>	<b>gs = 16.27*pHmin<sub>molt</sub> - 107.05</b>	<b>19.98</b>	<b>0.77</b>	<b>0.01</b>	7
molt60 <sub>10</sub>	gs = -4.81*pHmin <sub>molt</sub> + 51.49	25.74	0.47	0.09	7
molt60 <sub>20</sub>	gs = 0.19*NO3max <sub>molt</sub> + 8.99	25.74	0.47	0.09	7
<b>molt60<sub>30</sub></b>	<b>gs = 1.99*T<sub>molt</sub> - 2.75</b>	<b>20.70</b>	<b>0.74</b>	<b>0.01</b>	7
all30 <sub>10</sub>	gs = -0.012*pCO <sub>2</sub> min <sub>in-situ</sub> + 18.29	22.27	0.68	0.02	7
all30 <sub>20</sub>	gs = -0.012*pCO <sub>2</sub> min <sub>in-situ</sub> + 18.29	22.27	0.68	0.02	7
<b>all30<sub>30</sub></b>	<b>gs = 16.27*pHmin<sub>molt</sub> - 107.05</b>	<b>19.98</b>	<b>0.77</b>	<b>0.01</b>	7
<b>all30<sub>30</sub></b>	<b>gs = 1.16*Tmin<sub>molt</sub> + 9.65</b>	<b>20.04</b>	<b>0.77</b>	<b>0.01</b>	7
all60 <sub>10</sub>	gs = -0.012*pCO <sub>2</sub> min <sub>in-situ</sub> + 18.29	22.27	0.68	0.02	7
all60 <sub>20</sub>	gs = -0.012*pCO <sub>2</sub> min <sub>in-situ</sub> + 18.29	22.27	0.68	0.02	7
<b>all60<sub>30</sub></b>	<b>gs = 1.99*T<sub>molt</sub> - 2.75</b>	<b>20.70</b>	<b>0.74</b>	<b>0.01</b>	7

Overall best models are in bold.

experiments still provide information on whether a high pCO<sub>2</sub> environment affects the initial exoskeleton density of megalopae.

We μCT scanned a series pea crabs reared from zoeae to megalopae at ambient (400 μatm) and elevated (2800 μatm) pCO<sub>2</sub>. The zoeae were collected in light traps by Swinomish Tribal biologists at Coronet Bay in Puget Sound (48.398033, -122.628037) on June 3,

2019, then reared individually in well plates inside CO<sub>2</sub>-chambers at the NOAA Mukilteo Research Station. The CO<sub>2</sub> chambers and crab well plate culture methods are described in [McElhany et al. \(2022\)](#). Initially, 192 zoeae were partitioned equally into four CO<sub>2</sub> chambers (two replicate chambers per treatment). Chambers were maintained at 10°C with a 12 hour on/off light cycle. Zoeae were regularly fed

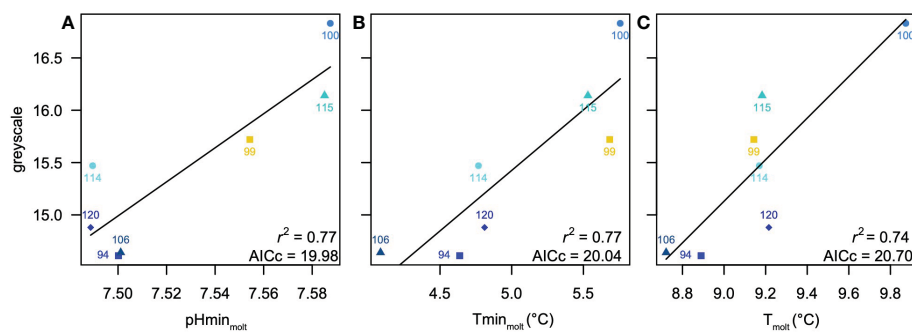


FIGURE 5

Summary of best models for the scenarios considered (Tables 2, 3) (A) greyscale density versus minimum pH at the time of z5-megalopae molt identified as optimal for molt30<sub>30</sub> and all30<sub>30</sub> scenarios, which also has the overall lowest AICc. (B) greyscale density versus minimum T at the time of z5-megalopae molt identified as nearly identical to the optimal model in molt30<sub>30</sub> and all30<sub>30</sub> scenarios (C) greyscale density versus temperature at the time of z5-megalopae molt identified as optimal for molt60<sub>30</sub> and all60<sub>30</sub> scenarios. Symbol colors indicate nearshore (cyan), intermediate (yellow) and offshore (blue) stations.

*Artemia salina* at a target concentration of 1 nauplius per milliliter every 3 days. Those zoeae that survived and molted to the megalope stage were maintained in culture for 14 days, which we considered to be long enough for them to experience any potential dissolution, but before they molted to juveniles. Approximately 14 days after molting, megalopae were preserved in 100% ethanol. A subset of the megalopae were used for  $\mu$ CT analysis (400  $\mu$ atm,  $n = 8$ ; 2800  $\mu$ atm  $n = 9$ ). We note that the optimal instrument parameters for *Pinnixa* sp. specimens were subtly different (55kV, 160 mA) than those for *M. magister* specimens so raw greyscale values are not directly comparable between the two species. However, because analyses were internally consistent for a given species, relative differences in integrated greyscale could still detect the direction of any density change.

## 3 Results

### 3.1 Exoskeleton density and optimal predictors in field-collected megalopae

$\mu$ CT greyscale values for field-collected megalopae are summarized in Table 1. Resolvable differences among the nine sites varied from a minimum of 13.93 at station 127 to a maximum of 16.83 at station 100. There was no obvious relationship between greyscale and latitude or distance from shore.

The best relationships between measured greyscale and environmental variables were always univariate, and are summarized in Table 3. Both int30 and int60 scenarios yielded modestly significant models (AICc = 26.70,  $r^2 = 0.5$ ,  $p = 0.03$ ), in which maximum DO was identified as the optimal predictor. Because maximum DO occurred shallower than 30 m, the regression equations and statistics are identical for both assumed habitat depths. DVM30<sub>xx</sub>, molt30<sub>10</sub> and molt30<sub>20</sub> scenarios all produced weak models (AICc = 27.90-28.89,  $r^2 = 0.17$ -0.28,  $p = 0.22$ -0.36) with inconsistent predictors. DVM60<sub>xx</sub>, molt60<sub>10</sub> and molt60<sub>20</sub> scenarios were stronger, but still only marginally significant (AIC = 23.33-25.28,  $r^2 = 0.47$ -0.60,  $p = 0.04$ -0.09). A molt30<sub>30</sub> model based on minimum pH at the time of molt was the strongest of any considered (AIC = 19.98,  $r^2 = 0.77$ ,  $p = 0.01$ ; Figure 5A), but a second model from this scenario based on minimum T at the time of molt performed nearly as well (AIC = 20.04,  $r^2 = 0.77$ ,  $p = 0.01$ ; Figure 5B). A molt60<sub>30</sub> model with T at the time of molt as an optimal predictor also performed well (AICc = 20.70,  $r^2 = 0.74$ ,  $p = 0.01$ ; Figure 5C).

Combining all possible predictors into a single pool in all30<sub>xx</sub> and all60<sub>xx</sub> scenarios selects minimum *in-situ*  $p\text{CO}_2$  at the site of collection as the optimal predictor (AICc = 22.27,  $r^2 = 0.68$ ,  $p = 0.02$ ) for molt times of 10 and 20 days (Table 3). Because minimum *in-situ*  $p\text{CO}_2$  occurs shallower than 30 m, both assumed depth habitats yield the same result. However, in cases where molt was assumed to occur 30 days prior to collection (i.e. all30<sub>30</sub> and all60<sub>30</sub> scenarios), results were identical to molt30<sub>30</sub> and molt60<sub>30</sub> scenarios, respectively. That is, the all30<sub>30</sub> scenario selected minimum pH at the time of molt, and the all60<sub>30</sub> scenario selected T at the time of molt. The AICc for the all30<sub>30</sub> model based on minimum T at the time of molt is only 0.06 higher than that for the optimal model based on minimum pH at the time of molt, suggesting it is only 3% less likely

and worthy of consideration. In summary, minimum pH at the time of molt assuming vertical migrations over the upper 30 m is the strongest overall predictor of greyscale density, but two alternate models based on minimum T at the time of molt (assuming migrations over the upper 30 m) and average T at the time of molt (assuming migrations over the upper 60 m) are also strong.

### 3.2 Comparison of exoskeleton density and dissolution

We find an insignificant correlation between exoskeleton density and semi-quantitative dissolution ( $r^2 = 0.27$ ,  $p = 0.23$ ), and only a marginal correlation with  $\Delta\Omega_{c-60}$  ( $r^2 = 0.50$ ,  $p = 0.03$ ). Consistent with this, the all60<sub>30</sub> scenario model based on  $\Delta\Omega_{c-60}$  has a  $\Delta\text{AICc}$  of 3.70, suggesting that the model based on T at the time of molt is about 6 times more likely than one based on  $\Delta\Omega_{c-60}$ . Similarly, the all30<sub>30</sub> scenario based on  $\Delta\Omega_{c-30}$  has a  $\Delta\text{AICc}$  of 6.02, implying that the model based on minimum pH at the time of molt is about 20 times more likely than one based on  $\Delta\Omega_{c-30}$ .

### 3.3 Exoskeleton density in culture experiments

The *Pinnixa* sp. crab were reared under controlled  $\text{CO}_2$  conditions for an average of 39 days (min = 23, max = 57), with an average time as zoeae of 26 days (min = 11, max = 46) and the average time as megalopae prior to sampling of 14 days (min = 11, max = 21). There was no statistical difference between the  $p\text{CO}_2$  treatments in the duration of zoea or megalope stage. However, three of the crabs in the low- $p\text{CO}_2$  treatment went through a zoeal molt (z4 to z5) then the molt to megalope (z5 to megalope), whereas all other crabs entered the experiment at the z5 stage and experienced only the z5 to megalope molt. The temperature in all chambers was constant with an overall mean of 10.0°C (s.d. = 0.2°C). Spectrophotometric pH values were not statically different among the replicate chambers, with mean low- $p\text{CO}_2$  treatment pH of 8.04 (s.d. = 0.05) and the mean high- $p\text{CO}_2$  treatment pH of 7.24 (s.d. = 0.03).  $\Omega_c$  calculated with seacarb.R (Gattuso et al., 2021) using pH and alkalinity input parameters was 2.55 (s.d. = 0.24) and 0.45 (s.d. = 0.03) for the low and high  $p\text{CO}_2$  treatments, respectively, with alkalinity based on site-specific salinity relationship described in Trigg et al. (2019). The greyscale value of 22.4 for pea crab megalopae reared from zoeae at the 2800 matm  $p\text{CO}_2$  treatment was effectively identical to the 22.3 measured in specimens from the 400 matm treatment, implying no significant change in exoskeleton density between the two  $p\text{CO}_2$  treatments.

## 4 Discussion

### 4.1 Effect of minimum pH at the time of zoea-megalope molt

Our evaluation of environmental controls on exoskeleton density suggests that conditions at the time of z5-megalope molt, 30 days prior to collection may be especially important. In particular,

minimum pH at the time of initial exoskeleton formation emerges as the single best predictor of exoskeleton density, and suggests that density increases by about 16 greyscale units per pH unit. The highest densities are associated with pH values that never fall below about 7.58 during the 24 hours assigned to z5-megalope molt using the DVM30 behavior, while stations where megalopae had lower-density exoskeletons (e.g. 94, 106, 114, and 120) typically exhibit minimum pH values of  $\sim 7.5$ . Hindcast trajectories suggest that low minimum-pH environments typically occur nearshore the western coast of Vancouver Island, but that there is no unique location for relatively high minimum pH values. For example, Figure 3 suggests that megalopae with denser exoskeletons collected at station 100 were more likely to molt from zoeae further offshore western Vancouver Island, while those at station 115 apparently molted mostly in the Salish Sea.

To our knowledge, no study has specifically investigated how environmental factors influence Dungeness crab megalope exoskeleton formation during the molt from zoea, but considerable work supports the plausibility of minimum pH being an important variable. Studies of larval crab survival and development at variable pH values often find higher mortality and slower progression through molt stages at lower pH or higher  $p\text{CO}_2$  conditions (Descôteaux, 2014; Schiffer et al., 2014; Miller et al., 2016; Giltz and Taylor, 2017; Gravinese et al., 2018; Reinhardt, 2020). Minimum values may be particularly important, and duration-dependent pH thresholds of 7.4 to 7.52 have been identified for larval decapods (Bednaršek et al., 2021), while a pH threshold of 7.43 has been suggested for the survival of blue crab zoea exposed to diel cycling (Tomasetti et al., 2021). A similar threshold response has been observed in juvenile blue king crab (*Paralithodes platypus*), which showed no change in growth or mortality at pH values of 7.8 and 8.1, but exhibited increased mortality and decreased growth at pH = 7.5 (Long et al., 2017). While we cannot be certain that exoskeleton density exhibits a threshold response to minimum pH, our lowest measured greyscale value of  $\sim 15$  corresponds to a minimum pH at the time of z5-megalope molt of  $\sim 7.5$  (Figure 5A) that is similar to previously identified thresholds, making it a plausible scenario. Regardless, it appears that the exoskeleton density of Dungeness megalopae are particularly sensitive to short-lived low pH extremes during the z5-megalope molt, and we suggest that greyscale density provides a metric for tracking the severity of those impacts.

The apparent link between minimum pH and exoskeleton density could reflect additional energetic costs at lower pH that may compromise a megalope's ability to precipitate its exoskeleton. Assuming studies of adult crab are applicable, the molt from z5 to megalope can be broadly divided into a pre-molt stage that includes the preparation for and actual shedding of the old cuticle, and a post-molt stage that consists of new exoskeleton mineralization. The pre-molt stage is characterized by active uptake of monovalent cations (e.g.  $\text{Na}^+$ ,  $\text{K}^+$ ), which drive an osmotic flux of water into the crab, resulting in large weight gains (Cameron, 1989). Calcium is passively transported across the gills and is stored to be used later during mineralization (Wheatly, 1999; Luquet and Marin, 2004; Luquet, 2012). Immediately after molting, the activity of Ca-ATPase enzymatic pumps and bicarbonate transporter proteins increase to actively bring calcium and bicarbonate into the cuticle (Cameron, 1989; Abehsera et al., 2021). Simultaneous active removal of protons from the cuticle promotes the conversion of bicarbonate to carbonate ion, thereby boosting cuticle  $\Omega_c$  and facilitating rapid calcite precipitation into a complex chitin-protein matrix (Cameron, 1985, 1989; Cameron and Wood, 1985; Luquet, 2012; Figure 6). Protons produced as a calcification byproduct must also be actively pumped away into the ambient seawater to prevent hemolymph acidosis (Cameron, 1985, 1989; Cameron and Wood, 1985; Henry et al., 2012).

The numerous instances of active transport involved in molting and reprecipitation of new exoskeleton (Figure 6) indicate it is an energy intensive process, and the energy required to reach a given cuticle  $\Omega_c$  would increase at lower ambient seawater pH values. For example, the presence of additional protons in ambient seawater at lower pH would mean more protons would need to be actively removed from the site of calcification to boost  $\Omega_c$  to the same degree of supersaturation, which would require additional energy. If this extra energy was not available, cuticle  $\Omega_c$  would decrease and may compromise exoskeleton formation. Considerable evidence suggests that coping with low pH conditions could require megalopae to divert energy to other functions thereby leaving less energy for active pumping and calcification and further compromising the ability to reach a given  $\Omega_c$ . While exposure to low pH or elevated  $p\text{CO}_2$  conditions has been shown to increase metabolism, oxygen consumption and ATP production in larval crabs (Schiffer et al., 2013; Trigg et al., 2019), this additional energy may disproportionately go to immune function (Niemisto et al., 2021). Similarly, juvenile isopods have been shown to reduce their carbonic anhydrase concentrations at high

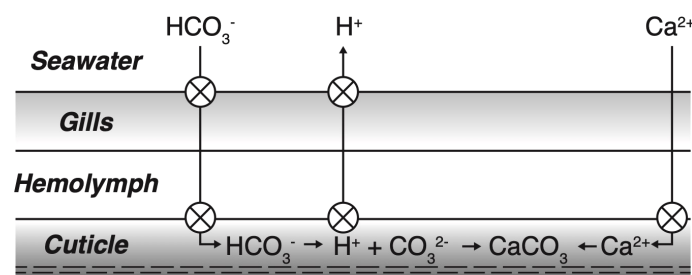


FIGURE 6

Illustration of post-molt calcification. Crossed circles indicate proposed locations of active transport requiring metabolic energy. Calcium is passively transported across the gills, but actively transported to the site of calcification in the cuticle. Bicarbonate is actively pumped both across the gills and to the site of calcification. Protons are actively pumped from the site of calcification to increase saturation state and remove protons produced during calcite precipitation. To maintain internal acid/base balance, protons are subsequently actively transported across the gills to ambient seawater. Adapted from Cameron, 1989.

$p\text{CO}_2$  conditions (Turner et al., 2016), which would decrease the efficiency of proton removal (Henry, 1984; Cameron and Wood, 1985) supporting the idea that exoskeleton formation is not a priority for energy expenditure at lower pH values.

When viewed collectively, a possible mechanism linking low pH to reduced exoskeleton density might be as follows: Energy limitations reduce the transport of calcium and bicarbonate to the site of exoskeleton precipitation, and reduce the removal of protons from it. Both contribute to a lower cuticle  $\Omega_c$ , which has been shown to decrease skeletal density and compromise crystal structures in other marine calcifiers (Cohen et al., 2009; Mollica et al., 2018). While additional work is required to confirm this specific hypothesis, it seems likely that an imbalance between the energy needed and the energy available for exoskeleton formation plays a prominent role in explaining the association between lower density exoskeleton and minimum pH at the time of z5-megalope molt.

## 4.2 Potential influence of temperature

Considerable evidence suggests that the net response of larval crabs to OA can vary due to interactions among other variables such as temperature, DO and food availability (e.g. Small et al., 2015; Gravinese et al., 2018; Trigg et al., 2019; Niemisto et al., 2021; Tomasetti et al., 2021). This is not surprising given that metabolism, respiration and other physiological processes are linked to energy balance, and thus the ability to cope with low pH conditions. While available evidence supports our selection of minimum pH at the time of z5-megalope molt as the most plausible single predictor of megalope exoskeleton density, models based on mean and minimum T at the time of z5-megalope molt also performed well and we further evaluate the importance of these variables.

Dungeness zoea appear to be adapted to temperatures between approximately 10–14°C, outside of which thermal stress can impact growth and development (Reed, 1969; Sulkin and McKeen, 1994, 1989), increase metabolism and carbohydrate consumption, and deplete lipid concentrations (Brown and Terwilliger, 1999; García-Guerrero et al., 2003; Green et al., 2014; Wittmann et al., 2018; Torres and Giménez, 2020). While most studies explore hyperthermal stress, hypothermal stress is also possible, and would generally leave less energy for exoskeleton formation, thereby potentially impacting exoskeleton density in a way similar to the pH mechanism described above. Our hindcast experiments indicate that all field-collected megalopae likely molted at mean temperatures below the optimal 10–14°C range, and experienced diel minima of 4.1 to 5.8°C, potentially making them more sensitive to low pH conditions. In light of this, it may be premature to attribute changes in megalope exoskeleton density exclusively to minimum pH at the time of z5-megalope molt, and minimum temperature may also be important.

## 4.3 Comparison with culture experiments

The suggestion that *M. magister* megalopae are sensitive to minimum pH is somewhat at odds with our *Pinnixa* sp. culture experiments, which show no change in exoskeleton density between

mean pH values of 7.24 and 8.04. While inter-species differences are a simple explanation for this apparent discrepancy, they are unsatisfying given the broad similarities between larval *M. magister* and *Pinnixa* sp. described above. Instead, we suggest the energy imbalance proposed to explain exoskeleton density variations among field-collected megalopae was minimized or eliminated by one or more experimental conditions, thereby allowing *Pinnixa* sp. exoskeleton formation to proceed relatively normally under both treatments.

A potential difference between field and cultured organisms was their access to food. Previous work suggests that unlimited access to prey can effectively eliminate thermal stress-induced mortality among zoeae and megalopae because it fuels compensatory responses that are too energetically costly under food limitation (Torres and Giménez, 2020). Cultured *Pinnixa* sp. were fed routinely, potentially providing sufficient energy for additional active pumping among zoeae in the high  $p\text{CO}_2$  treatment. This may have allowed these individuals to reach the same cuticle  $\Omega_c$  threshold during molt as the zoeae in the lower  $p\text{CO}_2$  treatment, thereby minimizing the influence of pH and allowing an exoskeleton of similar density to be precipitated. While the food available to field-collected *M. magister* at the time of z5-megalope molt is not known, it is plausible that they experienced greater food limitation and therefore a more significant response to pH.

Early life stage exposure history represents a variation on this idea that could also contribute to the apparent difference between *Pinnixa* sp. experiments and *M. magister* observations. In a study of pH carryover effects in Tanner crabs (*Chionoecetes bairdi*), Long et al. (2016) compared wild-brooded larvae to those derived from ovigerous females conditioned at pH values of 7.5, 7.8 and 8.1. Wild specimens transferred to low pH experimental conditions showed minimal effects, in much the same way as our *Pinnixa* sp. experiments. In contrast, larvae exposed to low pH since oogenesis had larger impacts on morphology, size, calcification and metabolic rate (Long et al., 2016). Based on this, it is possible that *M. magister* megalopae with lower density exoskeletons were not only exposed to suboptimal pH at the time of z5-megalope molt, but also prior to this time from oogenesis through zoeal stages. Such prolonged exposure may have depleted energy reserves, leaving little energy for the additional active pumping necessary to cope with low pH environments. On the other hand, if it is assumed that *Pinnixa* sp. were collected from an environment to which they were well adapted, their exposure to suboptimal pH in the experiments was brief and they may not have experienced such carryover effects. *Pinnixa* sp. may have entered experiments with energy reserves that facilitated additional active pumping and therefore no change in exoskeleton density. If correct, this possibility highlights the need for longer duration OA experiments that better capture carryover effects and will allow more realistic comparisons with field collected specimens.

Finally, minimum temperature is a noticeable difference between cultured *Pinnixa* sp. and field-collected *M. magister*. Mean temperatures inferred at the time of z5-megalope molt for field-collected *M. magister* varied from 8.6 to 10.2°C, and were similar to the nearly constant 10°C of culture experiments. However, inferred minimum temperatures for field-collected *M. magister* ranged from 4.1 to 5.8°C and were markedly cooler than any temperature experienced by *Pinnixa* sp. during the experiment. As discussed above, we cannot rule out the possibility that *M. magister* are sensitive to minimum temperature, and if this is the case, it may

explain why field-collected specimens exhibit an apparent sensitivity to pH that was not observed among cultured *Pinnixa* sp. This possibility suggests that additional experiments exploring how larval *M. magister* exoskeleton formation responds to hypothermal conditions during diel cycling could provide important insight into their overall sensitivity to environmental stressors.

#### 4.4 The relationship between exoskeleton density and dissolution

The weak correlation between exoskeleton greyscale density and dissolution, and the fact that  $\Delta\Omega_c$  was not selected as a top-

performing predictor during our model selection suggests that the two processes are not intimately linked. Instead, we suggest that  $\mu\text{CT}$ -based exoskeleton density and SEM-based dissolution severity represent complementary techniques that record responses at different life stages:  $\mu\text{CT}$ -based exoskeleton density is set by the conditions at the time of initial megalope exoskeleton formation while SEM-based dissolution severity measures subsequent environmental exposure between the time of exoskeleton formation and collection. Furthermore, the weak relationship between these variables implies either that dissolution does not preferentially remove exoskeleton of a certain density, or that the fraction of exoskeleton lost to dissolution is small, such that the initial density set at the time of z5-megalope molt is not influenced appreciably by subsequent dissolution.

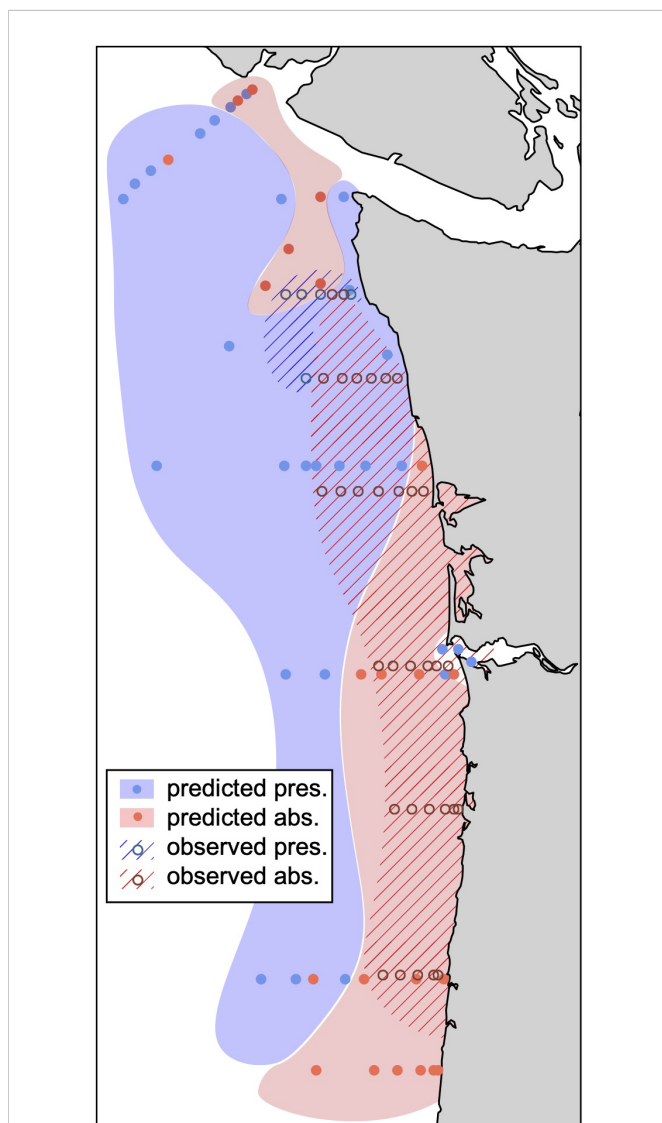


**FIGURE 7**  
Observed distribution of *M. magister* megalope presence (blue hatch, open circle) and absence (red hatch, open circle) from Morgan et al. (2019) compared with predicted presence (filled blue) and absence (filled red) in this study. Predictions use 30-day J-SCOPE hindcast simulations (see Methods) to calculate minimum pH at the time of z5-megalope molt for all northern California Current stations sampled during the 2016 WCOA cruise. The mean greyscale values of hypothetical megalopae at each site are then calculated using our best model (Table 3; Figure 5A) and predicted to be present or absent based on a greyscale threshold of 15.

#### 4.5 Comparison with population level data

The population-level response of *M. magister* megalope to environmental variables is ultimately most useful for informed management decisions. However, we cannot immediately assume that the individual megalope response to minimum pH at the time of z5-megalope molt translates to the population level. While constructing a robust relationship between individual- and population-level responses is not possible with our data set, we make a simple, initial evaluation. As discussed above, our lowest measured greyscale value of  $\sim 15$  equates to a pH of  $\sim 7.5$ , which represents a plausible threshold below which megalopae may not survive to be observed. If this is correct, and the population-level response is similar to that at the individual level, one would expect the regional distribution of megalope populations predicted from this greyscale threshold to resemble observations. To test this possibility, we used exposure history hindcasts for all WCOA 2016 stations within the JSCOPE domain to determine the minimum pH at their inferred z5-megalope molt locations, which were then linearly transformed into greyscale estimates using the optimal model from the all30<sub>30</sub> scenario (Table 3). Applying our proposed greyscale threshold value of  $\sim 15$ , we then predicted where megalopae would be present and absent.

Our predicted pattern of megalope distribution compares favorably to the observed distribution from 2009–2017 spring monitoring surveys (Morgan et al., 2019; Figure 7). While spatial domains do not perfectly overlap, both show megalopae are more likely to be present at more northerly and offshore sites, but are likely to be absent in more coastal and southern waters where pH at the time of z5 molt may fall below  $\sim 7.5$ . One exception is the Columbia River mouth where our simple threshold model erroneously predicts megalopae to be present. This may reflect additional controls on exoskeleton density or megalope presence-absence near low salinity terrestrial sources such as the Columbia River. Despite this shortcoming, the general similarity over much of the domain suggests that  $\mu\text{CT}$  based exoskeleton density has potential to inform population-level megalope responses, and therefore may be a valuable tool for making management decisions.

In addition, we suggest  $\mu\text{CT}$ -based exoskeleton density also has the potential to provide more nuanced information on *M. magister* populations impacted by environmental conditions including OA. For example, field surveys that find megalopae to be present, but with a greyscale density approaching our proposed threshold of 15, could

suggest a severely impaired population. Conversely, a location where megalopae are present and have appreciably higher greyscale values could reflect a significantly healthier population. By combining such field data with hindcast trajectories, it may also be possible to identify at-risk habitats thereby supporting more informed management decisions. For example, hindcast trajectories for populations with greyscale values near our threshold could identify locations of z5-megalope molt that are most likely to experience minimum pH values near or below 7.5. These regions could then receive special consideration when designing habitat monitoring programs.

## 5 Conclusion

To our knowledge, this is the first study to demonstrate resolvable differences in exoskeleton density among field-collected Dungeness crab megalopae using  $\mu$ CT. Exoskeleton density changes are best explained by variations in the minimum pH at the time of z5-megalope molt with higher densities being associated with higher minimum pH. We suggest that this relationship arises for two reasons associated with the energetic costs of exoskeleton formation. First, the higher concentration of protons in seawater at lower pH requires additional active pumping to reach a given cuticle  $\Omega_c$ , which would require additional energy. At the same time, less energy is available as it is diverted to other processes aimed at coping with a higher acidity environment. Minimum temperature at the time of z5-megalope molt also explains much of the variability in exoskeleton density implying that other environmental variables may interact to produce the observed density variations, and additional work is necessary to evaluate their relative influences.

Despite remaining uncertainties, minimum conditions at the approximate time of z5-megalope molt are routinely selected as the best predictors of exoskeleton density. This is noteworthy for two reasons. First, it highlights the importance of carryover effects and suggests that prior environmental conditions could have a large influence on the vitality of megalope populations. Given the connection between megalopae and adult populations (Shanks and Roegner, 2007; Park, 2012; Shanks, 2013), our results support efforts to consider the entire life cycle of *M. magister* when evaluating environmental impacts (e.g. Berger et al., 2021). Second, our result supports the importance of extreme events that might surpass critical thresholds as potentially being more important than mean conditions. Both results provide support for conducting additional culture experiments that rear *M. magister* from egg through all life stages, especially those that include realistic cycling across plausible maxima and minima (e.g. Tomasetti et al., 2021).

We establish  $\mu$ CT-based greyscale density as a promising metric of crab larvae condition that is more nuanced than simple presence-absence observations. While our conclusions are based on a relatively small sample size, available evidence generally supports their validity across the larger region. Additional analyses of field-collected specimens are still warranted however, especially considering the

potentially anomalous conditions associated with the North Pacific marine heatwave of 2016 (Bond et al., 2015). Such analyses should be readily achievable given that the method we describe is relatively fast, economical, and well-suited to high throughput measurements. With further refinement, we anticipate that  $\mu$ CT analyses will be a valuable addition to the suite of tools used to monitor the health of Dungeness crab larvae, thereby facilitating more informed management decisions related to the Dungeness crab fishery and more accurate model projections.

## Data availability statement

The original contributions presented in the study are included in the article/Supplementary Material. Further inquiries can be directed to the corresponding author.

## Author contributions

CS was the principal author of the manuscript, conducted  $\mu$ CT scans, and performed statistical tests with input from PE, SB, SS and EN. NB, SA and RF collected and processed biological samples, seawater geochemical data and ocean condition observations. SS, EN and AH designed and conducted particle tracking simulations. CS, PE, EN, SB, SS, SA, RF, AH and NB contributed to the writing and editing of the manuscript. All authors contributed to the article and approved the submitted version.

## Funding

We thank the NOAA Ocean Acidification Program for funding this work. Portions of this study were funded by the NOAA Northwest Fisheries Science Center. The contributions of SA and RF were supported by NOAA Pacific Marine Environmental Laboratory (PMEL) and the NOAA Ocean Acidification Program. This is PMEL contribution number 5314. NB acknowledges support from the Slovene Research Agency project # J12468.

## Acknowledgments

We thank Adam Summers for valuable discussions of  $\mu$ CT methods, Ian Inochs for comments on the manuscript, the Swinomish Tribe for collection of pea crab zoeae, and Kate Rovinski, Mike Maher and Danielle Perez for assisting in pea crab culture experiments. This work would not have been possible without the support of NOAA's Ocean Acidification Program, Pacific Marine Environmental Laboratory (PMEL) and Northwest Fisheries Science Center. This is PMEL contribution number 5314.

## Conflict of interest

The authors declare that the research was conducted in the absence of any commercial or financial relationships that could be construed as a potential conflict of interest.

## Publisher's note

All claims expressed in this article are solely those of the authors and do not necessarily represent those of their affiliated

organizations, or those of the publisher, the editors and the reviewers. Any product that may be evaluated in this article, or claim that may be made by its manufacturer, is not guaranteed or endorsed by the publisher.

## Supplementary material

The Supplementary Material for this article can be found online at: <https://www.frontiersin.org/articles/10.3389/fmars.2023.1095253/full#supplementary-material>

## References

- Abehsera, S., Bentov, S., Li, X., Weil, S., Manor, R., Sagi, S., et al. (2021). Genes encoding putative bicarbonate transporters as a missing molecular link between molt and mineralization in crustaceans. *Sci. Rep.* 11, 11722. doi: 10.1038/s41598-021-91155-w
- Akaike, H. (1974). A new look at the statistical model identification. *IEEE Trans. Autom. Control* 19, 716–723. doi: 10.1109/TAC.1974.1100705
- Alma, L., Kram, K. E., Holtgrieve, G. W., Barbarino, A., Fiamengo, C. J., and Padilla-Gamiño, J. L. (2020). Ocean acidification and warming effects on the physiology, skeletal properties, and microbiome of the purple-hinge rock scallop. *Comp. Biochem. Physiol. A. Mol. Integr. Physiol.* 240, 110579. doi: 10.1016/j.cbpa.2019.110579
- Bancroft, M. P. (2015). *An experimental investigation of the effects of temperature and dissolved oxygen on the growth of juvenile English sole and juvenile dungeness crab* (Oregon State University). Available at: <https://seagrant.oregonstate.edu/sgpubs/experimental-investigation-effects-temperature-and-dissolved-oxygen-growth-juvenile-english>.
- Ban, N. C., Eckert, L., McGreer, M., and Frid, A. (2017). Indigenous knowledge as data for modern fishery management: a case study of dungeness crab in pacific Canada. *Ecosyst. Health Sustain.* 3, 1379887. doi: 10.1080/20964129.2017.1379887
- Bednaršek, N., Ambrose, R., Calosi, P., Childers, R. K., Feely, R. A., Litvin, S. Y., et al. (2021). Synthesis of thresholds of ocean acidification impacts on decapods. *Front. Mar. Sci.* 8. doi: 10.3389/fmars.2021.651102
- Bednaršek, N., Feely, R. A., Beck, M. W., Alin, S. R., Siedlecki, S. A., Calosi, P., et al. (2020). Exoskeleton dissolution with mechanoreceptor damage in larval dungeness crab related to severity of present-day ocean acidification vertical gradients. *Sci. Total Environ.* 716, 136610. doi: 10.1016/j.scitotenv.2020.136610
- Bednaršek, N., Feely, R. A., Tolimieri, N., Hermann, A. J., Siedlecki, S. A., Waldbusser, G. G., et al. (2017). Exposure history determines pteropod vulnerability to ocean acidification along the US West coast. *Sci. Rep.* 7, 4526. doi: 10.1038/s41598-017-03934-z
- Berger, H. M., Siedlecki, S. A., Matassa, C. M., Alin, S. R., Kaplan, I. C., Hodgson, E. E., et al. (2021). Seasonality and life history complexity determine vulnerability of dungeness crab to multiple climate stressors. *AGU Adv.* 2(4), 19. doi: 10.1029/2021AV000456
- Bignami, S., Enochs, I. C., Manzello, D. P., Sponaugle, S., and Cowen, R. K. (2013). Ocean acidification alters the otoliths of a pantropical fish species with implications for sensory function. *Proc. Natl. Acad. Sci.* 110, 7366–7370. doi: 10.1073/pnas.1301365110
- Boßelmann, F., Romano Triguero, P., Fabritius, H.-O., Raabe, D., and Epple, M. (2007). The composition of the exoskeleton of two crustacea: The American lobster *homarus americanus* and the edible crab *pagurus*. *Thermochim. Acta* 463, 65–68. doi: 10.1016/j.tca.2007.07.018
- Bolze, J., Peng, B., Dingenouts, N., Panine, P., Narayanan, T., and Ballauff, M. (2002). Formation and growth of amorphous colloidal CaCO<sub>3</sub> precursor particles as detected by time-resolved SAXS. *Langmuir* 18, 8364–8369. doi: 10.1021/la025918d
- Bond, N. A., Cronin, M. F., Freeland, H., and Mantua, N. (2015). Causes and impacts of the 2014 warm anomaly in the NE pacific. *Geophys. Res. Lett.* 42, 3414–3420. doi: 10.1002/2015GL063306
- Brown, A. C., and Terwilliger, N. B. (1999). Developmental changes in oxygen uptake in cancer magister (Dana) in response to changes in salinity and temperature. *J. Exp. Mar. Biol. Ecol.* 241, 179–192. doi: 10.1016/S0022-0981(99)00071-4
- Burnham, K. P., and Anderson, D. R. (2010). *Model selection and multimodel inference: practical information-theoretic approach*. 2. ed (New York, NY: Springer).
- Burnham, K. P., Anderson, D. R., and Huyvaert, K. P. (2011). AIC model selection and multimodel inference in behavioral ecology: some background, observations, and comparisons. *Behav. Ecol. Sociobiol.* 65, 23–35. doi: 10.1007/s00265-010-1029-6
- Busch, D. S., and McElhany, P. (2016). Estimates of the direct effect of seawater pH on the survival rate of species groups in the California current ecosystem. *PLoS One* 11, e0160669. doi: 10.1371/journal.pone.0160669
- Cameron, J. N. (1985). Post-moult calcification in the blue crab (*Callinectes sapidus*): Relationships between apparent net h<sup>+</sup> excretion, calcium and bicarbonate. *J. Exp. Mar. Biol. Ecol.* 119, 275–285. doi: 10.1016/j.jeb.119.1.275
- Cameron, N. (1989). Post-moult calcification in the blue crab *callinectes sapidus*: timing and mechanisms. *J. Exp. Mar. Biol. Ecol.* 143, 285–304. doi: 10.1016/j.jeb.143.1.285
- Cameron, J. N., and Wood, C. M. (1985). Apparent h<sup>+</sup> excretion and CO<sub>2</sub> dynamics accompanying carapace mineralization in the blue crab (*Callinectes sapidus*) following moulting. *J. Exp. Mar. Biol. Ecol.* 114, 181–196. doi: 10.1016/j.jeb.114.1.181
- Contin, N. E., Cohen, A. L., Karnauskas, K. B., Tarrant, A. M., and McCorkle, D. C. (2010). Ocean warming slows coral growth in the central red Sea. *Science*. 329 (5989), 322–325. doi: 10.1126/science.1190182
- Carlstrom, D. (1957). The crystal structure of alpha-chitin (poly-N-acetyl-D-glucosamine). *J. Biophys. Biochem. Cytol.* 3, 669–683. doi: 10.1083/jcb.3.5.669
- Chan, F., Barth, J. A., Blanchette, C. A., Byrne, R. H., Chavez, F., Cheriton, O., et al. (2017). Persistent spatial structuring of coastal ocean acidification in the California current system. *Sci. Rep.* 7, 2526. doi: 10.1038/s41598-017-02777-y
- Chatzinikolaou, E., Grigoriou, P., Keklikoglou, K., Faulwetter, S., and Papageorgiou, N. (2017). The combined effects of reduced pH and elevated temperature on the shell density of two gastropod species measured using micro-CT imaging. *ICES J. Mar. Sci.* 74, 1135–1149. doi: 10.1093/icesjms/fsw219
- Chatzinikolaou, E., Keklikoglou, K., and Grigoriou, P. (2021). Morphological properties of gastropod shells in a warmer and more acidic future ocean using 3D micro-computed tomography. *Front. Mar. Sci.* 8. doi: 10.3389/fmars.2021.645660
- Chavez, F., Pennington, J. T., Michisaki, R., Blum, M., Chavez, G., Friederich, J., et al. (2017). Climate variability and change: Response of a coastal ocean ecosystem. *Oceanography* 30, 128–145. doi: 10.5670/oceanog.2017.429
- Christmas, A.-M. F. (2013). *Effects of ocean acidification on dispersal behavior in the larval stage of the dungeness crab and the pacific green shore crab* (Western Washington University). Available at: <https://cedar.wvu.edu/wwuet/306/>.
- Cohen, A. L., McCorkle, D. C., Putron, S., Gaetani, G. A., and Rose, K. A. (2009). Morphological and compositional changes in the skeletons of new coral recruits reared in acidified seawater: Insights into the biomineralization response to ocean acidification. *Geochim. Geophys. Res.* 14, 12. doi: 10.1029/2009GC002411
- Descôteaux, R. (2014). *Effects of ocean acidification on development of alaskan crab larvae (Thesis)* (University of Alaska Fairbanks). Available at: <https://scholarworks.alaska.edu/handle/11122/4532>.
- Di Santo, V. (2019). Ocean acidification and warming affect skeletal mineralization in a marine fish. *Proc. R. Soc B Biol. Sci.* 286, 20182187. doi: 10.1098/rspb.2018.2187
- Doney, S. C., Busch, D. S., Cooley, S. R., and Kroeker, K. J. (2020). The impacts of ocean acidification on marine ecosystems and reliant human communities. *Annu. Rev. Environ. Resour.* 45, 83–112. doi: 10.1146/annurev-environ-012320-083019
- Enochs, I. C., Manzello, D. P., Kolodziej, G., Noonan, S. H. C., Valentino, L., and Fabricius, K. E. (2016). Enhanced macroboring and depressed calcification drive net dissolution at high-CO<sub>2</sub> coral reefs. *Proc. R. Soc B Biol. Sci.* 283, 20161742. doi: 10.1098/rspb.2016.1742
- Feely, R. A., Alin, S. R., Carter, B., Bednaršek, N., Hales, B., Chan, F., et al. (2016). Chemical and biological impacts of ocean acidification along the west coast of north America. *Estuar. Coast. Shelf Sci.* 183, 260–270. doi: 10.1016/j.ecss.2016.08.043
- Feely, R. A., Byrne, R. H., Acker, J. G., Betzer, P. R., Chen, C.-T. A., Gendron, J. F., et al. (1988). Winter-summer variations of calcite and aragonite saturation in the northeast pacific. *Mar. Chem.* 25, 227–241. doi: 10.1016/0304-4203(88)90052-7
- Fordyce, A. J., Knuefing, L., Ainsworth, T. D., Beeching, L., Turner, M., and Leggat, W. (2020). Understanding decay in marine calcifiers: Micro-CT analysis of skeletal structures provides insight into the impacts of a changing climate in marine ecosystems. *Methods Ecol. Evol.* 11, 1021–1041. doi: 10.1111/2041-210X.13439

- García-Guerrero, M., Villarreal, H., and Racotta, I. S. (2003). Effect of temperature on lipids, proteins, and carbohydrates levels during development from egg extrusion to juvenile stage of *Cherax quadricarinatus* (Decapoda: Parastacidae). *Comp. Biochem. Physiol. A. Mol. Integr. Physiol.* 135, 147–154. doi: 10.1016/s1095-6433(02)00354-9
- Gattuso, J. P., Epitalon, J. M., Lavigne, H., and Orr, J. (2021). Seabarb: Seawater carbonate chemistry. *R package version 3.3.0*. doi: 10.5281/zenodo.4600014
- Giltz, S. M., and Taylor, C. M. (2017). Reduced growth and survival in the larval blue crab *Callinectes sapidus* under predicted ocean acidification. *J. Shellfish Res.* 36, 481–485. doi: 10.2983/035.036.0219
- Gosner, H. M. (2018). *Quantifying sensitivity and adaptive capacity of shellfish in the northern California current ecosystem to increasing prevalence of ocean acidification and hypoxia* (Oregon State University). Available at: <https://seagrant.oregonstate.edu/sgpubs/quantifying-sensitivity-and-adaptive-capacity-shellfish-northern-california-current-ecosystem>.
- Gravinese, P. M., Enochs, I. C., Manzello, D. P., and van Woesik, R. (2018). Warming and pCO<sub>2</sub> effects on Florida stone crab larvae. *Estuar. Coast. Shelf Sci.* 204, 193–201. doi: 10.1016/j.ecss.2018.02.021
- Gravinese, P. M., Enochs, I. C., Manzello, D. P., and van Woesik, R. (2019). Ocean acidification changes the vertical movement of stone crab larvae. *Biol. Lett.* 15, 20190414. doi: 10.1098/rsbl.2019.0414
- Green, B. S., Gardner, C., Hochmuth, J. D., and Linnane, A. (2014). Environmental effects on fished lobsters and crabs. *Rev. Fish Biol. Fish.* 2, 613–638. doi: 10.1007/s11160-014-9350-1
- Hauri, C., Gruber, N., McDonnell, A. M. P., and Vogt, M. (2013). The intensity, duration, and severity of low aragonite saturation state events on the California continental shelf. *Geophys. Res. Lett.* 40, 3424–3428. doi: 10.1002/grl.50618
- Henry, R. P. (1984). The role of carbonic anhydrase in blood ion and acid-base regulation. *Am. Zool.* 24, 241–251. doi: 10.1093/icb/24.1.241
- Henry, R. P., Lucu, C., Onken, H., and Weihrauch, D. (2012). Multiple functions of the crustacean gill: osmotic/ionic regulation, acid-base balance, ammonia excretion, and bioaccumulation of toxic metals. *Front. Physiol.* 3. doi: 10.3389/fphys.2012.00431
- Hobbs, R. C., and Botsford, L. W. (1992). Diel vertical migration and timing of metamorphosis of larvae of the dungeness crab *Cancer magister*. *Mar. Biol.* 112, 417–428. doi: 10.1007/BF00356287
- Hodgson, E. E., Kaplan, I. C., Marshall, K. N., Leonard, J., Essington, T. E., Busch, D. S., et al. (2018). Consequences of spatially variable ocean acidification in the California current: Lower pH drives strongest declines in benthic species in southern regions while greatest economic impacts occur in northern regions. *Ecol. Model.* 383, 106–117. doi: 10.1016/j.ecolmodel.2018.05.018
- Imm, J. (2015). "Effects of elevated CO<sub>2</sub> and decreased dissolved oxygen on phototactic behaviors of juvenile dungeness crab (*Cancer magister*)," in 2015 AGU Fall Meeting. Available at: <https://ui.adsabs.harvard.edu/abs/2016AGUOSAH54A0096J/abstract>.
- Iwasaki, S., Kimoto, K., Sasaki, O., Kano, H., and Uchida, H. (2019). Sensitivity of planktic foraminiferal test bulk density to ocean acidification. *Sci. Rep.* 9, 9803. doi: 10.1038/s41598-019-46041-x
- Johnson, R., Harianto, J., Thomson, M., and Byrne, M. (2020). The effects of long-term exposure to low pH on the skeletal microstructure of the sea urchin *Helicodidaris erythrogramma*. *J. Exp. Mar. Biol. Ecol.* 523, 151250. doi: 10.1016/j.jembe.2019.151250
- Long, W. C., Swiney, K. M., and Foy, R. J. (2016). Effects of high pCO<sub>2</sub> on tanner crab reproduction and early life history, part II: carryover effects on oogenesis and embryogenesis are stronger than direct effects. *ICES J. Mar. Sci.* 73, 836–848. doi: 10.1093/icesjms/fsv251
- Long, W. C., Van Sant, S. B., Swiney, K. M., and Foy, R. J. (2017). Survival, growth, and morphology of blue king crabs: effect of ocean acidification decreases with exposure time. *ICES J. Mar. Sci.* 74, 1033–1041. doi: 10.1093/icesjms/fsw197
- Lough, G. (1976). Larval dynamics of the dungeness crab, *Cancer magister*, off the central Oregon coast 1970–71. *Fish. Bull.* 74, 24.
- Luquet, G. (2012). Biomineralizations: insights and prospects from crustaceans. *ZooKeys* 176, 103–121. doi: 10.3897/zookeys.176.2318
- Luquet, G., and Marin, F. (2004). Biomineralisations in crustaceans: storage strategies. *Comptes Rendus Palevol. BIOMINERALISATION : DIVERSITE ET UNITE* 3, 515–534. doi: 10.1016/j.crpv.2004.07.015
- Magel, C. L., Lee, E. M. J., Strawn, A. M., Swieca, K., and Jensen, A. D. (2020). Connecting crabs, currents, and coastal communities: Examining the impacts of changing ocean conditions on the distribution of U.S. West coast dungeness crab commercial catch. *Front. Mar. Sci.* 7. doi: 10.3389/fmars.2020.00401
- Malick, M. J., Siedlecki, S. A., Norton, E. L., Kaplan, I. C., Haltuch, M. A., Hunsicker, M. E., et al. (2020). Environmentally driven seasonal forecasts of pacific hake distribution. *Front. Mar. Sci.* 7. doi: 10.3389/fmars.2020.578490
- Marshall, K. N., Kaplan, I. C., Hodgson, E. E., Hermann, A., Busch, D. S., McElhany, P., et al. (2017). Risks of ocean acidification in the California current food web and fisheries: ecosystem model projections. *Glob. Change Biol.* 23, 1525–1539. doi: 10.1111/gcb.13594
- McElhany, P., Busch, D. S., Lawrence, A., Maher, M., Perez, D., Reinhardt, E. M., et al. (2022). Higher survival but smaller size of juvenile dungeness crab (*Metacarcinus magister*) in high CO<sub>2</sub>. *J. Exp. Mar. Biol. Ecol.* 555, 151781. doi: 10.1016/j.jembe.2022.151781
- Mekkes, L., Renema, W., Bednaršek, N., Alin, S. R., Feely, R. A., Huisman, J., et al. (2021). Pteropods make thinner shells in the upwelling region of the California current ecosystem. *Sci. Rep.* 11, 1731. doi: 10.1038/s41598-021-81131-9
- Meng, Y., Guo, Z., Fitzer, S. C., Upadhyay, A., Chan, V. B. S., Li, C., et al. (2018). Ocean acidification reduces hardness and stiffness of the Portuguese oyster shell with impaired microstructure: a hierarchical analysis. *Biogeosciences* 15, 6833–6846. doi: 10.5194/bg-15-6833-2018
- Miller, J. J., Maher, M., Bohaboy, E., Friedman, C. S., and McElhany, P. (2016). Exposure to low pH reduces survival and delays development in early life stages of dungeness crab (*Cancer magister*). *Mar. Biol.* 163, 118. doi: 10.1007/s00227-016-2883-1
- Mollica, N. R., Guo, W., Cohen, A. L., Huang, K.-F., Foster, G. L., Donald, H. K., et al. (2018). Ocean acidification affects coral growth by reducing skeletal density. *Proc. Natl. Acad. Sci.* 115, 1754–1759. doi: 10.1073/pnas.1712806115
- Morgan, C. A., Beckman, B. R., Weitkamp, L. A., and Fresh, K. L. (2019). Recent ecosystem disturbance in the northern California current. *Fisheries* 44, 465–474. doi: 10.1002/fsh.10273
- Niemisto, M., Fields, D. M., Clark, K. F., Waller, J. D., Greenwood, S. J., and Wahle, R. A. (2021). American Lobster postlarvae alter gene regulation in response to ocean warming and acidification. *Ecol. Evol.* 11, 806–819. doi: 10.1002/ece3.7083
- Norton, E. L., Siedlecki, S., Kaplan, I. C., Hermann, A. J., Fisher, J. L., Morgan, C. A., et al. (2020). The importance of environmental exposure history in forecasting dungeness crab megalopae occurrence using J-SCOPE, a high-resolution model for the US Pacific Northwest. *Front. Mar. Sci.* 7. doi: 10.3389/fmars.2020.00102
- Ofstad, S., Zamelczyk, K., Kimoto, K., Chierici, M., Fransson, A., and Rasmussen, T. L. (2021). Shell density of planktonic foraminifera and pteropod species *Limacina helicina* in the barents Sea: Relation to ontogeny and water chemistry. *PLoS One* 16, e0249178. doi: 10.1371/journal.pone.0249178
- Pacific States Marine Fisheries Commission Fisher (2019). *Species report: Commercial land catch: Metric-tons (mt), revenue, and price-per-pound (Price/Lbs)* (Portland, OR: Pacific States Marine Fisheries Commission).
- Park, W.-G. (2012). Dynamics of adult and larval dungeness crabs: Larval abundance as an indicator of adult abundance in regional populations. *J. Fish. Mar. Sci. Educ.* 24, 9–17. doi: 10.13000/JFMSE.2012.24.1.009
- Rasmuson, L. K. (2013). The biology, ecology and fishery of the dungeness crab, *Cancer magister*. *Adv. Mar. Biol.* 65, 95–148. doi: 10.1016/B978-0-12-410498-3.00003-3
- Reed, P. H. (1969). Culture methods and effects of temperature and salinity on survival and growth of dungeness crab (*Cancer magister*) larvae in the laboratory. *J. Fish. Res. Board Can.* 26, 389–397. doi: 10.1139/f69-037
- Reinhardt, E. (2020). *The effects of ocean acidification on molt rate and carapace area in juvenile dungeness crabs (Cancer magister)* (Georgia Institute of Technology). Available at: <https://smartechn.gatech.edu/handle/1853/64840>.
- Richerson, K., Punt, A. E., and Holland, D. S. (2020). Nearly a half century of high but sustainable exploitation in the dungeness crab (*Cancer magister*) fishery. *Fish. Res.* 226, 105528. doi: 10.1016/j.fishres.2020.105528
- Saenger, C., Cohen, A. L., Oppo, D. W., Halley, R. B., and Carilli, J. E. (2009). Surface-temperature trends and variability in the low-latitude north Atlantic since 1552. *Nat. Geosci.* 2, 492–495. doi: 10.1038/ngeo552
- Saenger, C. P., and Evans, M. N. (2019). Calibration and validation of environmental controls on planktic foraminifera Mg/Ca using global core-top data. *Paleoceanogr. Paleoclimatol.* 34, 1249–1270. doi: 10.1029/2018PA003507
- Schiffer, M., Harms, L., Pörtner, H. O., Lucassen, M., Mark, F. C., and Storch, D. (2013). Tolerance of *Hyas araneus* zoea I larvae to elevated seawater pCO<sub>2</sub> despite elevated metabolic costs. *Mar. Biol.* 160, 1943–1953. doi: 10.1007/s00227-012-2036-0
- Schiffer, M., Harms, L., Pörtner, H., Mark, F., and Storch, D. (2014). Pre-hatching seawater pCO<sub>2</sub> affects development and survival of zoea stages of Arctic spider crab *Hyas araneus*. *Mar. Ecol. Prog. Ser.* 501, 127–139. doi: 10.3354/meps10687
- Shanks, A. L. (2013). Atmospheric forcing drives recruitment variation in the dungeness crab (*Cancer magister*), revisited. *Fish. Oceanogr.* 22, 263–272. doi: 10.1111/fog.12020
- Shanks, A. L., and Roegner, G. C. (2007). Recruitment limitation in dungeness crab populations is driven by variation in atmospheric forcing. *Ecology* 88, 1726–1737. doi: 10.1890/06-1003.1
- Siedlecki, S. A., Kaplan, I. C., Hermann, A. J., Nguyen, T. T., Bond, N. A., Newton, J. A., et al. (2016). Experiments with seasonal forecasts of ocean conditions for the northern region of the California current upwelling system. *Sci. Rep.* 6, 27203. doi: 10.1038/srep27203
- Small, D. P., Calosi, P., Boothroyd, D., Widdicombe, S., and Spicer, J. I. (2015). Stage-specific changes in physiological and life-history responses to elevated temperature and pCO<sub>2</sub> during the larval development of the European lobster *Homarus gammarus* (L.). *Physiol. Biochem. Zool.* 88, 494–507. doi: 10.1086/682238
- Sulkin, S. D., and McKeen, G. L. (1989). Laboratory study of survival and duration of individual zoeal stages as a function of temperature in the brachyuran crab *Cancer magister*. *Mar. Biol.* 103, 31–37. doi: 10.1007/BF00391062
- Sulkin, S. D., and McKeen, G. (1994). Influence of temperature on larval development of four co-occurring species of the brachyuran genus *Cancer*. *Mar. Biol.* 118, 593–600. doi: 10.1007/BF00347506
- Sulkin, S., Mojica, E., and McKeen, G. (2011). Elevated summer temperature effects on megalopal and early juvenile development in the dungeness crab, *Cancer magister*. *Can. J. Fish. Aquat. Sci.* 53, 2076–2079. doi: 10.1139/cjfas-53-9-2076
- Tomasetti, S. J., Kraemer, J. R., and Gobler, C. J. (2021). Brief episodes of nocturnal hypoxia and acidification reduce survival of economically important blue crab (*Callinectes sapidus*) larvae. *Front. Mar. Sci.* 8. doi: 10.3389/fmars.2021.720175

- Torres, G., and Giménez, L. (2020). Temperature modulates compensatory responses to food limitation at metamorphosis in a marine invertebrate. *Funct. Ecol.* 34, 1564–1576. doi: 10.1111/1365-2435.13607
- Trigg, S. A., McElhany, P., Maher, M., Perez, D., Busch, D. S., and Nichols, K. M. (2019). Uncovering mechanisms of global ocean change effects on the dungeness crab (*Cancer magister*) through metabolomics analysis. *Sci. Rep.* 9, 10717. doi: 10.1038/s41598-019-46947-6
- Turner, L. M., Ricevuto, E., Massa Gallucci, A., Lorenti, M., Gambi, M.-C., and Calosi, P. (2016). Metabolic responses to high pCO<sub>2</sub> conditions at a CO<sub>2</sub> vent site in juveniles of a marine isopod species assemblage. *Mar. Biol.* 163, 211. doi: 10.1007/s00227-016-2984-x
- Walther, K., Anger, K., and Pörtner, H. O. (2010). Effects of ocean acidification and warming on the larval development of the spider crab *hyas araneus* from different latitudes (54° vs. 79°N). *Mar. Ecol. Prog. Ser.* 417, 159–170. doi: 10.3354/meps08807
- Wheatly, M. G. (1999). Calcium homeostasis in crustacea: The evolving role of branchial, renal, digestive and hypodermal epithelia. *J. Exp. Zool.* 283, 620–640. doi: 10.1002/(SICI)1097-010X(19990601)283:7<620::AID-JEZ2>3.0.CO;2-3
- Wild, P. W. (1980). Effects of seawater temperature on spawning, egg development, hatching success, and population fluctuations of the dungeness crab. *Cancer magister* 21, 115–120.
- Wilks, D. S. (2006). *Statistical methods in the atmospheric sciences. 2nd ed* (Amsterdam ; Boston: Academic Press).
- Wittmann, A. C., Benrabaa, S. A. M., López-Cerón, D. A., Chang, E. S., and Mykles, D. L. (2018). Effects of temperature on survival, moulting, and expression of neuropeptide and mTOR signalling genes in juvenile dungeness crab (*Metacarcinus magister*). *J. Exp. Biol.* 221, jeb187492. doi: 10.1242/jeb.187492